On the approximation of a tesseroid by a rectangular prism

Michael Kuhn

School of Earth and Planetary Sciences and The Institute of Geoscience Research, Curtin University, Perth, Australia
E-Mail: M.Kuhn@curtin.edu.au

Abstract

In global gravity forward modelling the tesseroid is commonly used as elementary mass element. However, formulas for the gravitational potential and its derivatives currently suffer from numerical problems when evaluating in its close proximity. Based on the subdivision of a tesseroid in smaller rectangular prisms, this study examines the gravitational field in the close proximity of a tesseroid including its faces, edges, vertices and interior and quantifies approximation errors when replaced by a single rectangular prism. Results show that approximation errors can exceed 100 μGal when placing the computation point at the vertex of a $30'' \times 30'' \times 10$ km tesseroid but considerably reduce for smaller tesseroids and when placing the computation point at the tesseroid's centre top face. While this study confirms that the prism is a suitable mass element to model masses in close proximity of the evaluation point it also opens further research questions.

1 Introduction

Gravity field modelling frequently requires the calculation of gravitational effects induced by given masses (e.g. Heiskanen and Moritz, 1967). In space-domain this is usually done through the application of numerical integration techniques or replacement of the mass distribution by an envelope of regularly shaped mass elements such as point masses, prisms or tesseroids. For this approach, approximation errors depend on how well the real mass distribution is expressed by the discrete mass elements.

While local mass distributions may be modelled in planar approximation using rectangular prisms (hereafter called prisms) for regional and global applications the curvature of the Earth has to be considered. In this case a spherical or ellipsoidal volume element e.g. tesseroid (also called spherical or ellipsoidal prism) together with constant or variable mass density, can be considered as a *natural* mass element (e.g. Anderson, 1976; Grüninger, 1990; Heck and Seitz, 2007). However, as pointed out by e.g. Heck and Seitz (2007), for the tesseroid, no closed formula solutions for the gravitational potential and its derivatives exist.

To mitigate this problem, solutions have been proposed based on Taylor series expansions of the respective integral kernels in spherical (e.g. Heck and Seitz, 2007; Wild-Pfeiffer, 2008; Deng et al., 2016) or Cartesian (e.g. Grombein et al., 2013) coordinates. It has been demonstrated that these solutions, termed here in general as tesseroid formulas, provide accurate and numerically efficient estimates when the computation point is located some distance away from the source masses, e.g. the tesseroid (Grombein et al., 2013). For computation points located in close proximity of a tesseroid, on its faces, edges or vertices or the interior the evaluation of the tesseroid formulas shows significant numerical problems, e.g. the near area problem. The mitigation of these problems require some alternate modelling such as numerical integration

Erschienen bei KIT Scientific Publishing
Schriftenreihe des Studiengangs
Geodäsie und Geoinformatik 2018,1

DOI Einzelbeitrag:
10.5445/KSP/1000080231

Festschrift zur Verabschiedung von
Prof. Dr.-Ing. Dr. h.c. Bernhard Heck
(Schw)Ehre, wem (Schw)Ehre gebührt

DOI Festschrift:
10.5445/KSP/1000080324

Dieses Werk ist lizenziert unter einer Creative Commons Namensnennung - Weitergabe unter gleichen Bedingungen 4.0 International Lizenz (CC BY-SA 4.0): https://creativecommons.org/licenses/by-sa/4.0/deed.en

(e.g. Wild-Pfeiffer, 2008; Roussel et al., 2015; Uieda et al., 2016), the use of different mass elements such as prisms (e.g. Heck and Seitz, 2007) and/or subdivision of the tesseroid (e.g. Heck and Seitz, 2007; Grombein et al., 2013). In this regard the prism can provide a suitable replacement when evaluating directly on the topographic surface even in spherical or ellipsoidal approximation (e.g. Kuhn et al., 2009; Hirt et al., 2016).

Several studies have examined approximation errors when replacing a tesseroid by a mass-equal prism of identical vertical extension (e.g. Anderson, 1976; Grüninger, 1990; Kuhn, 2000; Heck and Seitz, 2007; Wild-Pfeiffer, 2008). Apart from some selected evaluation points only, none has yet attempted to examine the entire gravitational field in the very close proximity of a tesseroid, the space where either the use of tesseroid formulas lead to numerical problems or numerical integration techniques become increasingly intensive (e.g. Ku, 1977; Wild-Pfeiffer, 2008; Roussel et al., 2015; Uieda et al., 2016). Based on the concept of subdividing a tesseroid in smaller prisms, this study intends to examine the gravitational field generated by a tesseroid in its very close proximity including its faces, edges, vertices and interior. Particular focus will be on approximation errors in gravitational attraction when replacing a tesseroid by a mass-equal prism.

2 Methodology

2.1 Approximation of a tesseroid by a prism

The term tesseroid has been introduced by Anderson (1976) describing a spherical (or ellipsoidal) volume element. In spherical approximation it is bounded by the respective surface pairs related to the geographic longitudes λ_1 and λ_2, latitudes ϕ_1 and ϕ_1 and radii R_1 and R_2 (cf. Figure 2.1). In this study the tesseroid is approximated by a prism following the basic idea introduced by Anderson (1976). Hereby the tesseroid is approximated such that the prism (i) has the same volume, (ii) is aligned with the axes of the topocentric coordinate system x', y', z' and (iii) has an identical vertical extension , e.g., $\Delta H = R_2 - R_1 = \Delta z$. Here the axes x', y', z' are aligned with the north, east and radial directions through the tesseroid's geometric centre Q_0, respectively (cf. Figure 2.1 and 2.2, and point notations used therein). The geometric centre is defined as $\lambda_0 = \frac{\lambda_1+\lambda_2}{2}$, $\phi_0 = \frac{\phi_1+\phi_2}{2}$, $R_0 = \frac{R_1+R_2}{2}$.

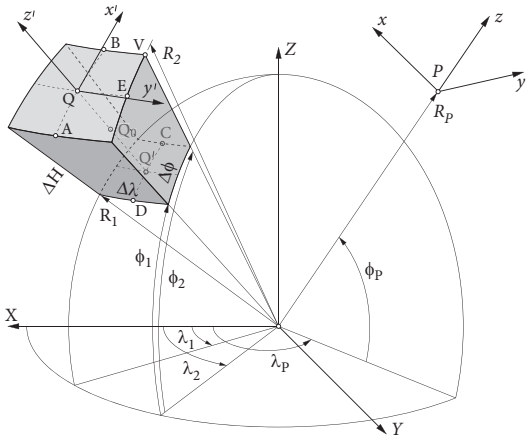

Figure 2.1: A tesseroid in spherical approximation.

Based on the above approximation, the prism, in comparison to the tesseroid, has a different geometry and as such a different mass distribution. This change is exemplified in Figure 2.2 illustrating a cross sectional view (along the meridian through point Q or Q_0) of a tesseroid ($ABCD$) approximated by a mass-equal prism ($A'B'C'D'$). Shaded in grey are the "wedge-like" masses that are displaced.

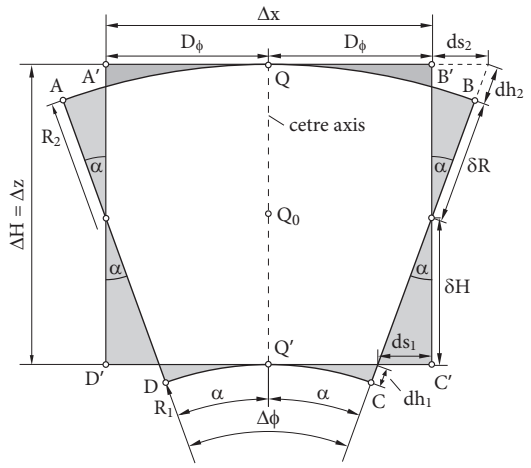

Figure 2.2: Approximation of a tesseroid by a prism shown as cross section along the meridian through Q.

Here the position of the prism is chosen so that its geometric centre is identical to that of the tesseroid. This implies that there are no mass displacements at the centre of the tesseroid's top face (point Q) where often the computation point is located. This particular choice, however, leads to a slight separation between the centroids of the tesseroid and prism. Based on the equivalence of mass and vertical extension, the horizontal dimension of the prism expressed along the

local north-south (x') and east-west (y') directions are given as (e.g. Anderson, 1976)

$$\Delta x = 2D_\phi = R\Delta\phi \tag{2.1}$$

$$\Delta y = 2D_\lambda = R_C \cos\phi_0 \Delta\lambda \tag{2.2}$$

with the mean radius $R = R_0$ and $\Delta\lambda = \lambda_2 - \lambda_1$, $\Delta\phi = \phi_2 - \phi_1$. Anderson (1976) points out that in Eq. 2.2 the radius of the centroid R_C can safely be replaced by R leading to a first-order approximation of the mass (Heck and Seitz, 2007). As an example, the relative approximation error is $\approx 1.2\ 10^{-7}$ for the volume of a tesseroid with $\Delta\lambda = \Delta\phi = 5'$ and $\Delta H = 10\ km$.

Based on the geometric relations in Figure 2.2 distances ds_i and $dh_i (i = 1,2)$, expressing geometric differences between tesseroid and prism, are given as

$$ds_1 = D_\phi - R_1 \tan\alpha, \quad ds_2 = R_2 \tan\alpha - D_\phi \tag{2.3}$$

$$dh_i = R_i \left(\frac{1-\cos\alpha}{\cos\alpha} \right), \quad i = 1,2\,. \tag{2.4}$$

Further the dimensions of the "wedge-like" masses are characterised by D_ϕ (cf. Eq. 2.1) and

$$\delta H = \frac{ds_1}{\tan\alpha} \quad \text{and} \quad \delta R = \frac{ds_2}{\sin\alpha} - dh_2\,. \tag{2.5}$$

In order to provide some quantification of the displaced masses at the upper edge of the tesseroid (e.g. point B), Table 2.1 lists the distances D_ϕ, ds_2, dh_2, and δR for selected horizontal dimensions (DEM resolutions) and a tesseroid height of $\Delta H = 10\ km$.

Table 2.1: Distances D_ϕ, ds_2, dh_2, and δR at the upper edge of a tesseroid with a horizontal dimension $\Delta\lambda \times \Delta\phi$ and height of 10 *km* centred at the equator (e.g. $\phi_0 = 0^o$). Mean Earth radius is $R = 6,378,130\ m$. Units in $[m]$.

$\Delta\lambda \times \Delta\phi$	D_ϕ	ds_2	dh_2	δR
$5' \times 5'$	4,638.312	3.637	1.688	4,999.438
$30'' \times 30''$	463.831	0.364	0.017	4,999.994
$3'' \times 3''$	46.383	0.036	<0.001	5,000.000
$1'' \times 1''$	15.461	0.012	<0.001	5,000.000

Results in Table 2.1 show that the displaced masses can be considerable for tesseroids with a horizontal dimension of $30'' \times 30''$ or larger and become very small or negligible for smaller dimensions.

2.2 Gravitational attraction of a tesseroid

Unlike for other elementary mass elements (e.g. point mass or prism) no closed analytical formulas can be provided for the gravitational potential and its derivatives for a tesseroid as elliptic integrals need to be solved (Heck and Seitz, 2007). As outlined in the introduction, solution strategies based on Taylor series expansions lead to numerical problems when the computation point is located in close proximity of the tesseroid (Heck and Seitz, 2007). Therefore, as this is the area of interest here, an alternative technique has to be used to derive reference values for the gravitational effects.

In this study the method of subdividing the tesseroid horizontally and vertically into $n_\lambda \times n_\phi \times n_H$ smaller mass elements is used where n_λ, n_ϕ and n_H indicate the number of subdivisions in longitude, latitude and radial directions, respectively. This is a common method to improve gravity calculations in close proximity of the source masses (e.g. Forsberg, 1984; Heck and Seitz, 2007; Grombein et al., 2013). Following this approach the original tesseroid is approximated by smaller tesseroids which in this study are further replaced by mass-equal prisms (cf. Section 2.1).

The use of prisms has the advantage that the respective formulas provide precise numerical values for the gravitational potential and first derivatives at any location including its faces, edges, vertices or interior (cf. Nagy et al., 2000, 2002). Here, the subdivision is iteratively increased as long as the difference between two subdivision steps falls below a given threshold ε (e.g. $\varepsilon < 1\ \mu Gal$). While this criterion is rather simple it serves the purpose of obtaining reference values. More sophisticated criteria to stop the iteration (based on point masses) are provided by, e.g., Uieda et al. (2016) and cited references therein.

In order to numerically demonstrate the convergence of the subdivision procedure using prisms, Figure 2.3 shows the differences in gravitational attraction δg_z (in radial direction) between subsequent subdivision steps for selected evaluation points at the tesseroid's top face. In all instances the procedure seems to numerically converge, e.g. differences get gradually smaller.

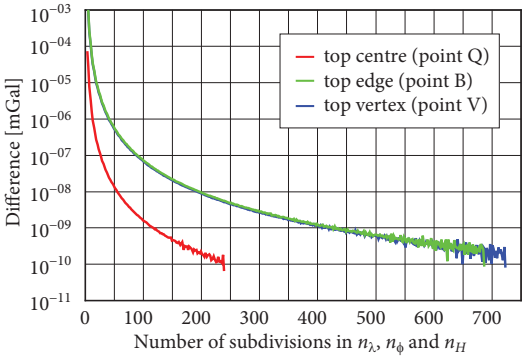

Figure 2.3: Differences in gravitational attraction δg_z between subsequent subdivisions (horizontal and vertical) of a $30'' \times 30'' \times 10\ km$ tesseroid. The iteration has been stopped at $\varepsilon = 10^{-10}\ mGal$ ($10^{-15}\ ms^{-2}$).

While the test above only reveals that the procedure numerically converges to some value it does not guarantee that it converges to the *correct* value. In order to test the latter the same procedure is applied to model δg_z of a spherical shell, e.g. for each tesseroid forming the complete spherical shell the same subdivision procedure is applied. Results shown in Table 2.2 for various horizontal resolutions clearly demonstrate that increased subdivision (e.g. smaller threshold ε) considerably reduces the absolute and relative errors, e.g. indicating that the procedure converges towards the correct value, at least within the given precision levels.

Table 2.2: Absolute (upper value) and relative (lower value) errors in gravitational attraction δg_z of a spherical shell ($R = 6,378,130\ m$, $\Delta H = 10\ km$). Errors are the differences between the analytical solution and result of the subdivision procedure. Evaluation is on the shell's top surface. Units of absolute errors in [μGal].

$\Delta\lambda \times \Delta\phi$	$n/a^{(1)}$	$1\ mGal^{(2)}$	$1\ \mu Gal^{(2)}$	$1\ nGal^{(2)}$
$1^\circ \times 1^\circ$	6,925.742	705.349	54.012	4.404
	3.1e-3	3.2e-4	2.4e-5	2.0e-6
$15' \times 15'$	751.638	39.870	13.393	1.606
	3.4e-4	1.8e-5	6.0e-6	7.2e-7
$5' \times 5'$	-107.991	-6.972	-5.182	-1.088
	4.8e-5	3.1e-6	2.3e-6	4.5e-7

(1) No subdivision. (2) Each tesseroid forming the complete shell is subdivided by at least $3 \times 3 \times 3$ elements with further subdivisions applied as required to reach the indicated threshold levels ε.

2.3 Gravitational attraction of a prism

As outlined in Section 2.2 this study uses prisms to derive the gravitational effect of a tesseroid through subdivision (cf. Section 2.2) as well as to replace the original tesseroid (cf. Section 2.1). Formulas to derive the gravitational potential and its derivatives for a prism are well-known and can be found in e.g. Mader (1951), Nagy (1966) and Nagy et al. (2000, 2002). Here the numerically more stable formulas given by e.g. Grüninger (1990), Kuhn (2000) and Heck and Seitz (2007) are used and hereafter referred to as prism formulas.

Using the prism formulas the gravitational attraction at the computation point P (e.g. gravity vector components $\delta g'_x$, $\delta g'_y$, $\delta g'_z$) can directly be derived in the topographic coordinate system (x', y', z') aligned with the prism edges (cf. Figure 2.4).

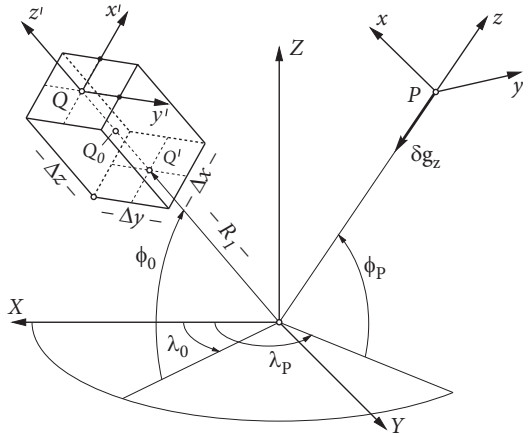

Figure 2.4: Gravitational attraction δg_z of a prism in spherical approximation.

However, in spherical or ellipsoidal approximation an additional transformation needs to be applied to obtain the gravitational attraction aligned with the axes of the topocentric coordinate system (x, y, z) at P (cf. Figure 2.4). This can be done through a rotation matrix relating the base vectors of the two topocentric coordinate systems via the base vectors of the geocentric coordinate system (X, Y, Z), (cf. Grüninger, 1990; Kuhn, 2000; Heck and Seitz, 2007).

3 Numerical study

This section provides an insight into the gravitational field of a tesseroid and its approximation by a mass-equal prism. Specific focus is on the gravitational attraction in radial direction δg_z, evaluated in the very close proximity of the tesseroid. In order to avoid numerical problems of the tesseroid formulas, reference values for δg_z are obtained by iterative subdivision as outlined in Section 2.2. Approximation er-

rors are derived by comparison of the reference values with δg_z, obtained when replacing the tesseroid by a mass-equal prism (cf. Section 2.1) without using any subdivision. All numerical tests are done in spherical approximation using $R = 6,378,137\ m$, mean density $\rho = 2670\ kg\ m^{-3}$ and Newton's gravitational constant $G = 6.672 \cdot 10^{-11} m^3\ kg^{-1} s^{-2}$. Further, the respective geometrical centres of the tesseroids used are located at $\lambda_0 = \phi_0 = 0^o$ and $R_0 = R$.

3.1 Approximation errors at selected locations

Before studying the gravitational field in close proximity of the tesseroid approximation errors are derived at the following two locations:

(a) At the centre of the tesseroid's top face (cf. point Q in Figure 2.1).

(b) At the north-eastern vertex of the tesseroid (cf. point V in Figure 2.1).

While point Q can be considered as a commonly used evaluation point on the topographic surface (also examined by Heck and Seitz (2007) and Grombein et al. (2013)), point V provides an example for a location close to major mass displacements (cf. Figure 2.2). Therefore, larger errors can be expected at the latter location. Tables 3.1 and 3.2 list the respective approximation errors in relation to horizontal and vertical tesseroid dimensions commonly used to model source masses close to the computation point.

The results show that the approximation errors at Q are relatively small reaching magnitudes above the μGal-level for the largest height of 10 km only. A maximum error of 30 μGal (relative 5.410^{-4}) is obtained for the largest tesseroid dimension of $30'' \times 30'' \times 10\ km$. These relatively low approximation errors are due to the fact that the bulk of the displaced masses are some distance away from the computation point. However, this is not anymore the case when the computation point is either located at an edge or vertex as can be seen by considerably larger approximation errors in Table 3.2. Now the approximation error is mostly above the μGal-level and smaller only for the smallest tesseroid dimensions considered. For the largest tesseroid dimension of $30'' \times 30'' \times 10\ km$ the approximation error is now 109 μGal (relative 4.0 10^{-3}). Overall, it can be noticed that most approximation errors (absolute and relative) are at least one order of magnitude higher when evaluating at the vertex of the tesseroid rather than at the centre top face.

Table 3.1: Absolute (upper values) and relative (lower values) approximation errors in gravitational attraction δg_z at the centre of the tesseroid's top face (cf. point Q). Units of the absolute approximation errors in [μGal].

$\Delta\lambda \times \Delta\phi$	$\Delta H = 100\ m$	$\Delta H = 1\ km$	$\Delta H = 10\ km$
$30'' \times 30''$	0.300	0.116	30.583
	2.9e-5	2.6e-6	5.4e-4
$5'' \times 5''$	0.003	0.406	6.928
	5.0e-7	4.3e-5	7.2e-4
$1'' \times 1''$	0.005	0.124	1.461
	2.5e-6	6.4e-5	7.5e-4

Table 3.2: Same as Table 3.1 but at the upper north-eastern vertex of the tesseroid (cf. point V).

$\Delta\lambda \times \Delta\phi$	$\Delta H = 100\ m$	$\Delta H = 1\ km$	$\Delta H = 10\ km$
$30'' \times 30''$	2.218	11.052	109.100
	8.3e-4	6.6e-4	4.04e-3
$5'' \times 5''$	0.228	2.218	19.936
	1.1e-4	5.0e-4	4.1e-3
$1'' \times 1''$	0.050	0.486	4.068
	6.3e-5	5.14e-4	4.2e-3

3.2 Approximation errors on the top face

In this experiment the gravitational attraction δg_z and approximation errors (absolute and relative) are examined on and in close proximity of the tesseroid's top face. The evaluation is done on part of the sphere with radius R_2 including and extending around the tesseroid's top face (cf. Figure 3.1 A). Panel B in Figure 3.1 illustrates δg_z of a tesseroid with the dimensions of $30'' \times 30'' \times 1\ km$. It can be seen that largest values are present on top of the tesseroid (maximum at centre) and quickly reduce with distance from the tesseroid. While lines of equal gravitational attraction very close to the tesseroid follow to some extent its shape they take on a near circular shape when extending further away from the tesseroid. This behaviour shows that at some distance from the tesseroid the gravitational field more and more resembles that of a

point mass, e.g. the impact of edges becomes negligible. This is consistent with the 1st order approximation of the tesseroid formulas expressing the gravitational field of a point mass (cf. Heck and Seitz, 2007).

Analysing the approximation errors (cf. Figure 3.1 C) it can be seen that maximum errors are present at the vertices and edges, e.g. locations of largest mass displacements (cf. Section 2.1). Confirming results from Section 3.1, at the centre top face of the tesseroid approximation errors are relatively small. Form the vertices and edges approximation errors quickly reduce to levels well below the μGal level. At a distance of about ½ the horizontal dimension of the tesseroid (e.g. $15''$) approximation errors are close to zero and change their sign from positive to negative and further away start to slightly increase in magnitude, though remain below the μGal level.

In terms of relative approximation errors (cf. Figure 3.1 D) again the vertices and edges show largest values with magnitudes reaching almost 0.1% (see also Table 3.2). Like the absolute approximation errors also the relative errors reduce rather quickly to minimum values at a distance of about ½ the tesseroid's horizontal dimension and slightly increase again to a level of about 0.002% further away.

3.3 Approximation errors in the meridian plane

In this experiment the gravitational attraction and approximation errors are examined in the vertical cross section along the meridian through the geometric centre of the tesseroid (cf. Figure 3.2 A). This includes locations on the north-south faces and interior of the tesseroid. Panel B in Figure 3.2 illustrates the gravitational attraction with maximum positive values at the centre top face (see also Section 3.2) gradually tapering off with increased height and horizontal distance. The behaviour is almost symmetrical (though with opposite sign) to the mean sphere with radius R passing through the geometrical centre of the tesseroid (e.g. zero height). Therefore, maximum negative values are present at the centre bottom face of the tesseroid and zero gravity occurs close to the sphere with radius R.

Approximation errors shown in Figure 3.2 C again show largest (positive) magnitudes at the edges of the tesseroid as could already be seen in Figure 3.1 C. Negative approximation errors are mostly present inside the tesseroid and extending to the north and south of the tesseroid faces. Interestingly there are small areas of negative approximation errors between the edges (large positive errors) and centre top/bottom faces (small positive errors). These can be explained by the deviation between the top/bottom faces of the tesseroid and prism (cf. Figure 2.2). While approximation errors are always positive on the top/bottom faces of the tesseroid (cf. Figure 3.1 C) they rapidly become negative as the computation point is elevated/lowered from these surfaces. The transition from positive to negative values happens over the approximate distance that separates both surfaces, which for small-sized tesseroids can happen over only few *mm*. Again approximation errors quickly reduce to sub-μGal levels with distance from the tesseroid.

Relative approximation errors (cf. Figure 3.2 D) show similar behaviour to their absolute counterparts at and above/below the top/bottom faces. Again rather large relative errors are present at the edges and much smaller at the centres of the tesseroid's top and bottom faces consistent with the relative errors shown in Figure 3.1 D. However, maximum relative errors are present on and close to the sphere with radius R and to some extend along the faces of the tesseroid. This behaviour is related to the fact that δg_z is close to zero around the mean sphere (cf. Figure 3.2 D) and as such even small absolute approximation errors can lead to rather large relative errors.

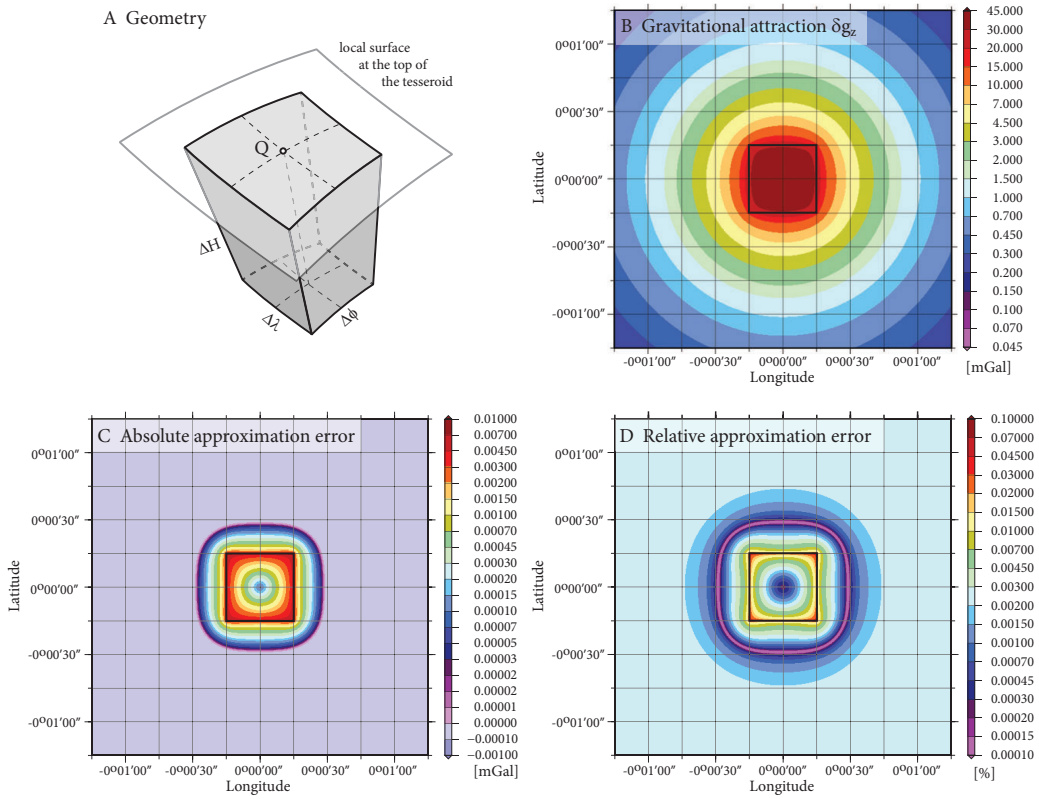

Figure 3.1: Gravitational attraction and approximation errors on and in close proximity of the tesseroid's top face. The thick black line indicates the extension of the tesseroid with a dimension of $30'' \times 30'' \times 1\ km$. Colour scales are non-linear.

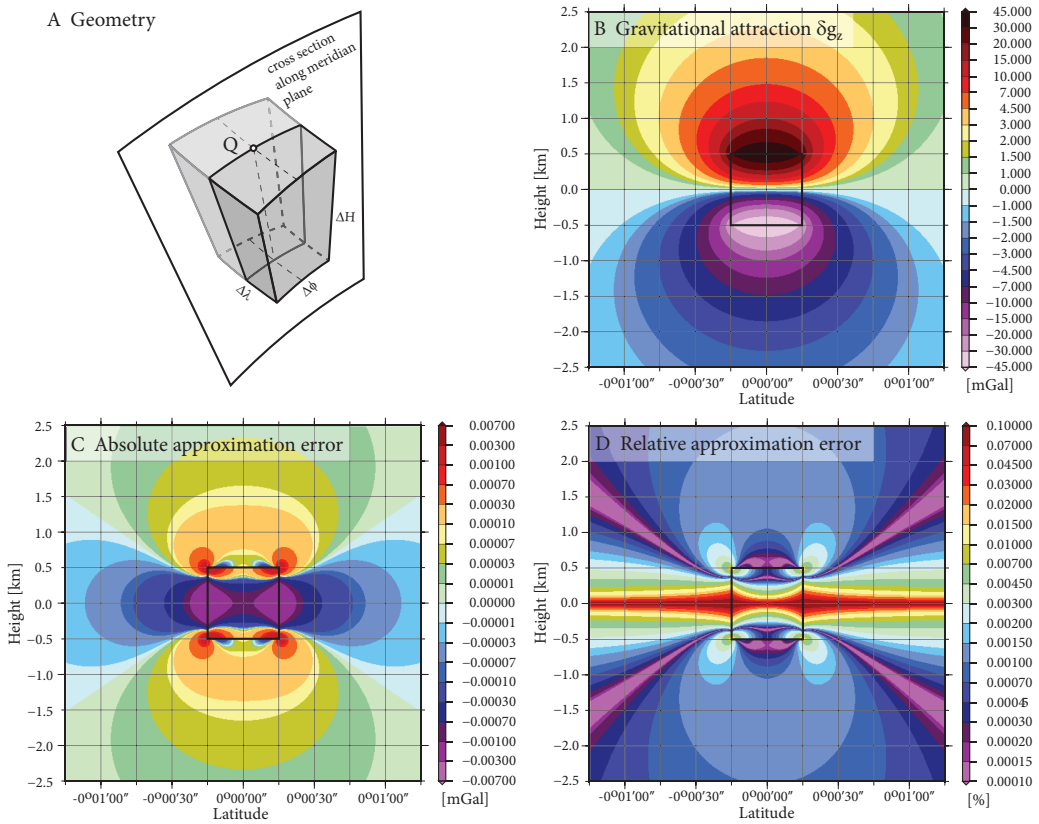

Figure 3.2: Gravitational attraction and approximation errors in the meridian plane through the tesseroid's geometric centre. The thick black line indicates the extension of the tesseroid with a dimension of $30'' \times 30'' \times 1\ km$. Colour scales are non-linear.

4 Discussion and Conclusions

This study provided insight into the gravitational field in very close proximity of a tesseroid including its edges, vertices, faces and interior. Particular focus was on approximation errors when replacing a tesseroid by a mass-equal prism. While providing some quantifications in this regards, several new research questions may arise from the results as outlined further in this section.

It has been demonstrated that horizontal and vertical subdivision of a tesseroid and subsequent replacement of the smaller mass elements by mass-equal prisms is a viable procedure to obtain precise reference values for the gravitational attraction of a tesseroid. This enabled the evaluation of the gravitational field in the very close proximity of the tesseroid, the space where the evaluation with tesseroid formulas currently leads to numerical problems. This also validates Heck and Seitz (2007), proposing that prisms should be used close to the computation point.

As a main outcome, it has been shown that approximation errors in the close proximity of the tesseroid largely vary depending on the selected location of the computation point. This behaviour is directly related to spatially varying mass changes associated to the replacement of the tesseroid by a mass-equal prism. Depending on the horizontal and vertical dimension of the tesseroid maximum errors mostly well above the μGal level are present when the computation point is located at or close to the vertices (similarly at the edges, not shown), e.g. areas close to considerable mass changes (cf. Section 2.1). On the other hand approximation errors (absolute and relative) are in almost all cases at least one order of magnitude smaller when the computation point is located at the centre of the tesseroid's top face. In this case approximation errors stay well below the μGal level for all but the largest tesseroid dimension ($30' \times 30' \times 10\ km$) considered. This underlines the importance of a careful selection of the computation point location when aiming to minimize approximation errors in the very close proximity of the tesseroid.

Apart from the careful selection of the computation point location in gravity forward modelling, approximation errors could further be reduced by subdividing the tesseroid (or tesseroids) in close proximity of the computation point as has been demonstrated by the successful derivation of reference values for the gravitational attraction of a tesseroid. While this study uses prisms others have explored the use of different mass elements to be used in the subdivision process (e.g. Wild-Pfeiffer, 2008; Grombein et al., 2013; Uieda et al., 2016). In this regard, a question still to be answered is which elementary mass element may be best suited both in terms of accuracy and numerical efficiency when aiming to evaluate in the very close proximity of the tesseroid including its edges, vertices, faces and interior. For example, while numerically more intensive, prism have the advantage that "mass-free" areas are kept to a minimum (mostly at edges and vertices) while point masses may have larger "mass-free" areas. This would make prisms better candidates when evaluation in the interior of the tesseroid is required, e.g. for the modelling of plumblines. Another benefit of the subdivision procedure, not explored further in this study, might be the possibility to provide precision estimates for global gravity forward modelling estimates when accounting for discretisation errors that arise from the use of a particular mass element (e.g. rectangular prism vs. tesseroid). As such the subdivision procedure could be employed to evaluate approximation errors for any type of mass element (e.g. point mass, mass line, mass surface, polyhedron, etc.). Such studies may become more important when aiming at regional and global gravity forward modelling at the highest possible precision level, e.g. μGal or below but still be able to perform calculations in a reasonable timeframe.

This study examines a rather benign case in terms of the tesseroid's location at the equator where the tesseroid has a near quadratic base. In this case approximation errors, when replacing a tesseroid by a prism, may be at a minimum (e.g. Heck and Seitz, 2007). Further studies in terms of the tesseroid's location are warranted to study the respective gravitational fields in relation to the geographic latitude. While the horizontal dimension in longitude direction, e.g. D_λ (cf. Eq. 2.2 in Section 2.1), of the prism will account for the meridian convergence it is to be expected that larger errors are present at higher latitudes.

Finally, when examining discretisation errors arising from geometric approximations of elementary mass elements one important aspect not considered here is the

question of how good do these represent the real mass distribution (e.g. topography)? It is well know that for example flat-topped tesseroids or prisms may be a rather crude approximation of the real (undulating) topography (e.g. Smith et al., 2001). While several solution strategies have been suggested (e.g. inclined top, polyhedral, bi-cubic interpolation) more comprehensive studies in relation to global high-resolution topographic masses have not yet been undertaken but may explain current μGal discrepancies when comparing high-resolution gravity forward modelling of the Earth's global topography in the space and frequency domains (e.g. Hirt and Kuhn, 2014; Hirt et al., 2016).

Acknowledgements

Supercomputing resources were kindly provided by Western Australia's Pawsey Supercomputing Centre.

Thank You:

A very special thank you goes to Prof Bernhard Heck who was the driving force some two decades ago in sparking my interest in gravity forward modelling in general and the use of prisms in particular. I am indebted to Bernhard's invaluable guidance during my diploma and PhD theses.

References

Anderson, E. G. (1976): The effect of topography on solutions of Stokes' problem. Unisurv S-14, Report. School of Surveying, University of New South Wales, Australia.

Deng, X.-L., Grombein, T., Shen, W.-B., Heck, B., and Seitz, K. (2016): Corrections to "A comparison of the tesseroid, prism and point-mass approaches for mass reductions in gravity field modelling" (Heck and Seitz, 2007) and "Optimized formulas for the gravitational field of a tesseroid" (Grombein et al., 2013). *Journal of Geodesy* 90(6):585–587. DOI: 10.1007/s00190-016-0907-8.

Forsberg, R. (1984): A study of terrain reductions, density anomalies and geophysical inversion methods in gravity field modelling. Report 355. Department of Geodetic Science and Surveying, The Ohio State University, Columbus, USA.

Grombein, T., Seitz, K., and Heck, B. (2013): Optimized formulas for the gravitational field of a tesseroid. *Journal of Geodesy* 87(7):645–660. DOI: 10.1007/s00190-013-0636-1.

Grüninger, W. (1990): Zur topographisch-isostatischen Reduktion der Schwere. PhD thesis. Universität Karlsruhe, Germany.

Heck, B. and Seitz, K. (2007): A comparison of the tesseroid, prism and point-mass approaches for mass reductions in gravity field modelling. *Journal of Geodesy* 81(2):121–136. DOI: 10.1007/s00190-006-0094-0.

Heiskanen, W. A. and Moritz, H. (1967): Physical geodesy. W. H. Freeman & Co., San Francisco, USA.

Hirt, C. and Kuhn, M. (2014): Band-limited topographic mass distribution generates full-spectrum gravity field: gravity forward modeling in the spectral and spatial domains revisited. *Journal of Geophysical Research* 119(4):3646–3661. DOI: 10.1002/2013JB010900.

Hirt, C., Reußner, E., Rexer, M., and Kuhn, M. (2016): Topographic gravity modelling for global Bouguer maps to degree 2,160: Validation of spectral and spatial domain forward modelling techniques at the 10 microgal level. *Journal of Geophysical Research* 121(9):6846–6862. DOI: 10.1007/s00190-015-0857-6.

Ku, C. C. (1977): A direct computation of gravity and magnetic anomalies caused by 2- and 3-dimensional bodies of arbitrary shape and arbitrary magnetic polarization by equivalent-point method and a simplified cubic spline. *Geophysics* 42(3):610–622. DOI: 10.1190/1.1440732.

Kuhn, M. (2000): Geoidbestimmung unter Verwendung verschiedener Dichtehypothesen. *Deutsche Geodätische Kommission, Reihe C*, no. 520. Verlag der Bayerischen Akademie der Wissenschaften in Kommission beim Verlag C. H. Beck, Munich, Germany.

Kuhn, M., Featherstone, W. E., and Kirby, J. F. (2009): Complete spherical Bouguer gravity anomalies over Australia. *Australian Journal of Earth Science* 56(2):213–223. DOI: 10.1080/08120090802547041.

Mader, K. (1951): Das Newtonsche Raumpotential prismatischer Körper und seine Ableitungen bis zur dritten Ordnung. *Österreichische Zeitschrift für Vermessungswesen*, *Sonderheft* 11.

Nagy, D., Papp, G., and Benedek, J. (2000): The gravitational potential and its derivatives for the prism. *Journal of Geodesy* 74(7–8):552–560. DOI: 10.1007/s001900000116.

Nagy, D., Papp, G., and Benedek, J. (2002): Corrections to *The gravitational potential and its derivatives for the prism*. *Journal of Geodesy* 76(8):475. DOI: 10.1007/s00190-002-0264-7.

Nagy, D. (1966): The gravitational attraction of a right rectangular prism. *Geophysics* 31(2):362–371. DOI: 10.1190/1.1439779. URL: +%20http://dx.doi.org/10.1190/1.1439779.

Roussel, C., Verdun, J., Cali, J., and Masson, F. (2015): Complete gravity field of an ellipsoidal prism by Gauss-Legendre quadrature. *Geophysical Journal International* 203(3):2220–2236. DOI: 10.1093/gji/ggv438. URL: http://dx.doi.org/10.1093/gji/ggv438.

Smith, D. A., Robertson, D. S., and Milbert, D. G. (2001): Gravitational attraction of local crustal masses in spherical coordinates. *Journal of Geodesy* 74(11–12):783–795. DOI: 10.1007/s001900000142.

Uieda, L., Barbosa, V. C. F., and Braitenberg, C. (2016): Tesseroids: Forward-modeling gravitational fields in spherical coordinates. *Geophysics* 81(5):41–48. DOI: 10.1190/geo2015-0204.1. URL: https://doi.org/10.1190/geo2015-0204.1.

Wild-Pfeiffer, F. (2008): A comparison of different mass elements for use in gravity gradiometry. *Journal of Geodesy* 82(10):637–653. DOI: 10.1007/s00190-008-0219-8.